Part No. 2, 4th QTR

7.7-10.1.5.1
CR-152651

AGRESTE

(E77-10151) AGRESTE PROGRAMME. PART 2: N77-22580
FRENCH TEST SITES Progress Report, Jul. -
Dec. 1976 (Centre d'Etude Spatiale des
Rayonnements) 41 p HC A03/MF A01 CSCL 05B Unclas
G3/43 00151

PROGRAMME

Original photography may be purchased from:
EROS Data Center
10th and Dakota Avenue
Sioux Falls, SD 57198

PROGRESS REPORT

JULY - DECEMBER 1976

28790

PART 2

FRENCH TEST-SITES

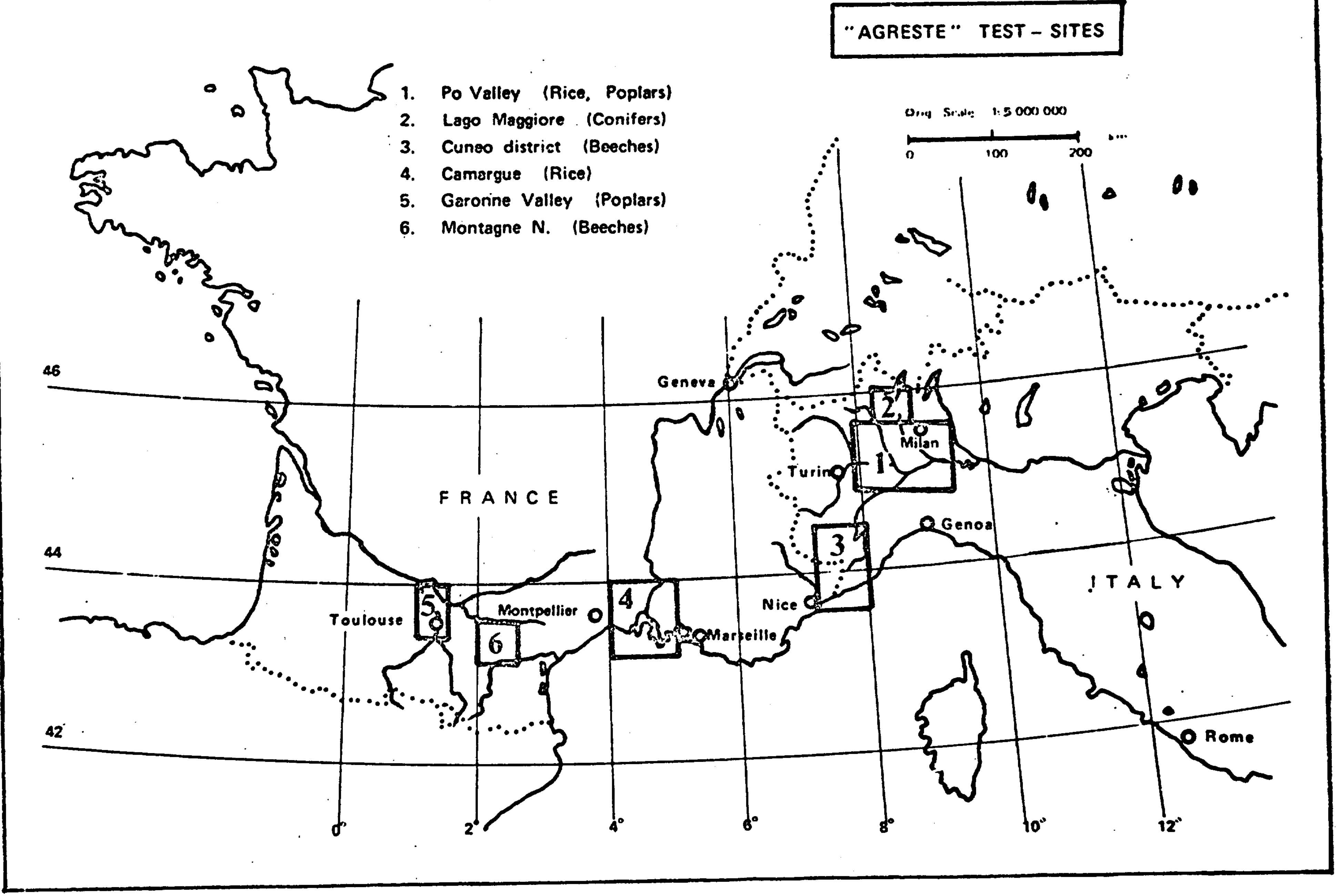
"AGRESTE" TEST - SITES
1. Po Valley (Rice, Poplars)
2. Lago Maggiore (Conifers)
3. Cuneo district (Beeches)
4. Camargue (Rice)
5. Garonne Valley (Poplars)
6. Montagne N. (Beeches)
0
100
200
46
44
42
0°
2°
4°
6°
8°
10°
12°
FRANCE
ITALY
Geneva
Milan
Turin
Genoa
Nice
Marseille
Montpellier
Toulouse
Rome
1
2
3
4
5
6

The quaterly report of the french part of the AGRESTE program presents the summaries of some results obtained during July-December 1976 period.

On rice-site (AGRESTE test-site n° 4), the study leads to use two kinds of methods on data processing of Landsat 2 and photographic imageries : the first on several classification algorithms and the second on edges detection.

On poplar site (AGRESTE test-site n° 5), two works are carried out : the use of analytic inventory to do a quantitative forecast of usefull timber for next years on a large area and the use of biometric connections to do a quantitative estimation of the timber volume in a given field.

G. FLOUZAT
Technical Manager

CONTENTS

CHAPTER I

INVENTORY AND AVAILABLE TIMBER FORECAST

IN A POPLAR AREA

by G. FLOUZAT*

Abstract

In this paper, the quantitative analysis of a poplar map gives the number of fields, the planted surfaces and the percent of cover-classes by map-sections. These results are completed by a ground sampling which shows the age and the cultivar nature of poplar fields. This enables to make a quantitative forecast of the global available timber and of the available timber for every cultivated variety.

I - BACKGROUND

In a first "Quaterly Report" (December 1975-January 1976), the methodology of poplars mapping was presented. It consists in the recognition of age-classes by connection with cover-classes identified on infra-red color photographs (IRC, fligt : 01.05.1975). Four classes of trees cover/soil surfaces ratio are used :

First class (I) = from 0 to 5 %

Secondth class (II) = from 5 to 25 %

Third class (III) = from 25 to 75 %

Fourth class (IV) = more than 75 %

*** Centre d'Etude Spatiale des Rayonnements**
9, Avenue du Colonel Roche
31029 TOULOUSE CEDEX

They are recognized by photointerpretation and with automatic interpretation helps like theoritical model digitalized by a microdensitometer.

The figure of following page shows the poplars cartography obtained in a representative part of the test-site n° 5 of AGRESTE programme by this method. The scale of the map is 1/100 000 but the original work is on 1/20 000e. The used IRC photographs have a scale of 1/10 000.

II - EXPLOITATION OF THE MAP

At the same time during which a study was carried out by the Department of Agriculture, this map was used for several accounts to be compared with statistics of the Government Services. These operations affected the four sections of the cartography for three aims :

- quantitative inventory of the fields number (Table I)
- quantitative inventory of planted surfaces (Table II)
- classes percentages in each sections (Table III)

The following three tables present these results.

III - GLOBAL FORECASTING OF AVAILABLE TIMBER

Forecasting of available timber is established with results of the map study. It is "global" because all cultivated varieties are counted without discrimination. A representative sounding with ground data on the considered area determines the relations between plantation age and classes identified by remote sensing. Figure 1gives these correspondances where m is the mean age and s the standard deviation of the four classes.

To realize the global forecast, the following bases are used with figure 1 :

- timber product of class IV will be cut during the 6 years after remote sensing date
- plantations age of class III covers 6 years
- plantations age of class II covers 3 years
- plantations age of class I covers 3 years.

Simultaneous, IRC photographs permit to measure plantation density on the 4 classes, that leads to an evaluation of the corresponding number of trees.

POPLARS MAP OF THE SOUTH PART OF THE AGRESTE TEST-SITE n° 5

Scale : 1/100.000

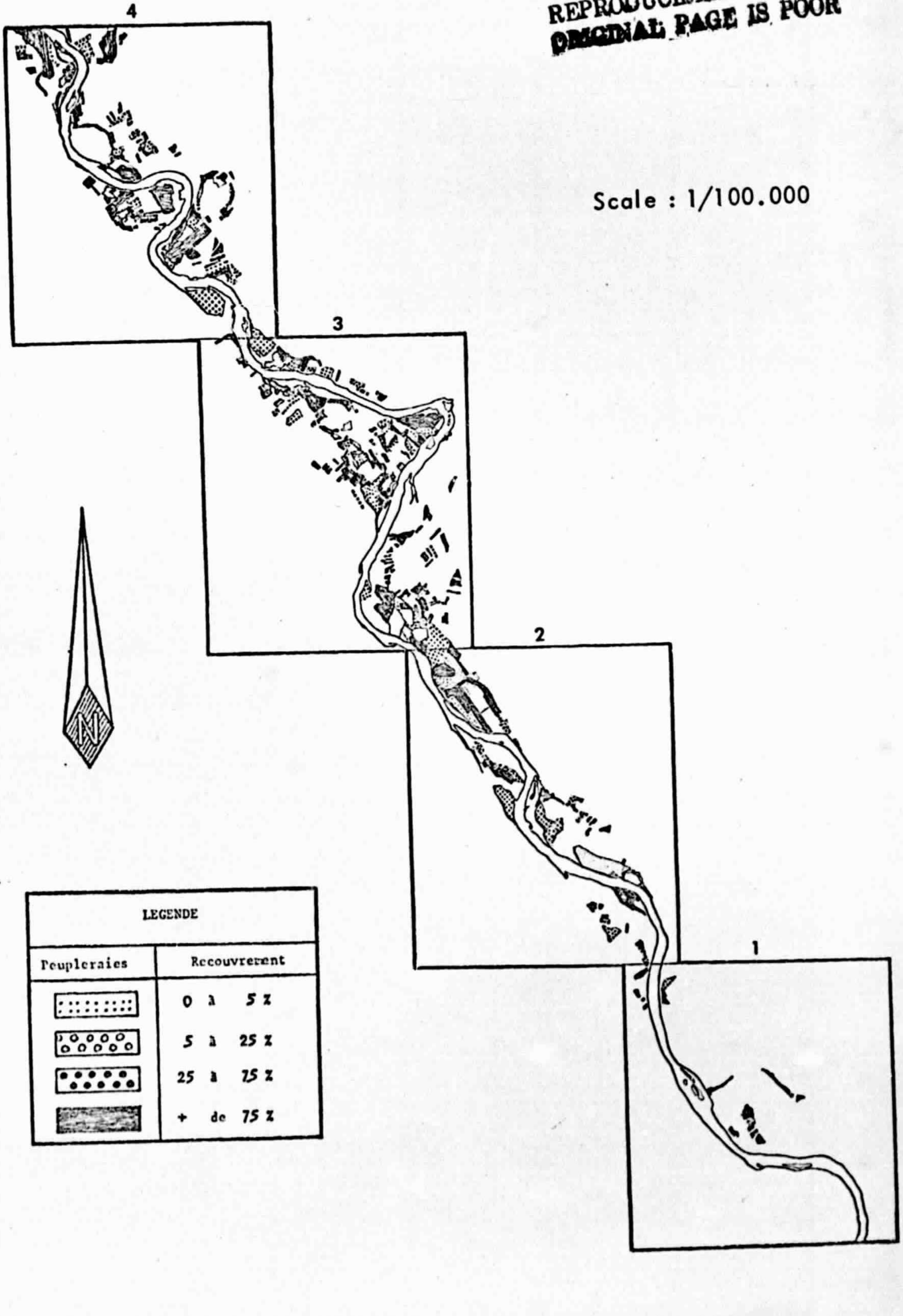

TABLE I = FIELDS NUMBERS

Sections \ Classes	I	II	III	IV	Total	%
1	0	1	3	14	18	4,2
2	10	14	17	27	68	15,8
3	22	24	50	97	193	44,7
4	13	15	37	87	152	35,3
Total	45	54	107	225	431	100
%	10,4	12,5	24,8	52,2	100	

TABLE II = POPLARS SURFACES (ha)

Sections \ Classes	I	II	III	IV	Total	%
1	0	1,68	3,12	13,44	18,24	3,3
2	34,44	27,76	36,44	50,92	149,56	27,2
3	28,64	21,64	49,48	100,56	200,32	36,4
4	10,88	34,72	36,16	100,80	182,56	33,1
Total	73,96	85,80	125,20	265,72	550,68	100
%	13,4	15,6	22,7	48,2	100	

TABLE III : PERCENTAGES OF SURFACES

Sections \ Classes	I	II	III	IV	Total
1	0	9,2	17,1	73,7	100
2	23,0	18,6	24,4	34,0	100
3	14,3	10,8	24,7	50,2	100
4	5,9	19,0	19,8	55,2	100

TABLE IV : PERCENTAGES OF THE DIFFERENT CULTIVATED VARIETIES

Cultivars \ Classes	I	II	III	IV	Total
I 214 (I)	5,1	5,1	12,3	25,4	47,9
Robusta (R)	2,2	1,4	11,6	17,4	32,6
Mixte (I) + (R)	2,9	0	5,1	3,6	11,6
45 - 51	1,4	1,4	0	0	2,8
Divers	1,4	0	2,2	1,4	5,0

Therefore, these data contain the global forecasting shown in figure 2 where usable surfaces in four time periods are presented for 18 years after the remote sensing.

In addition, the figure 3 gives surfaces and trees numbers which will be cut every years during the same time.

IV - FORECASTING OF USABLE TIMBER FOR EACH CULTIVATED VARIETY

With data from the Regional Forestry Services and with ground data, a sounding was made to know the percent of fields occuped by the different cultivated varieties.

The table IV gives results for the mapped region. It shows that the representation of two cultivated varieties (I 214 and Robusta) is more than 80 % of the plantations in this area.

The sounding noted also the cover-class obtained from IRC imagery. Therefore, their time-repartition leads to establish different forecasts (figures 4, 5 and 6) for the different cultivated varieties with the same base as global forecasting.

V - CONCLUSION

The results show that the available timber is decreasing after 1980. It seems that this comes from the corn extension since about ten years in the same ecological conditions. However, a certain recovery of planting exists since a few years.

This methodology study presents two interesting aspects = it is fast and covers all the region (naturaly, it is a little less accurate than ground inventories) and it is possible to be generalized for all poplars plantations.

Therefore, it can be considered like a future tool for land-planning.

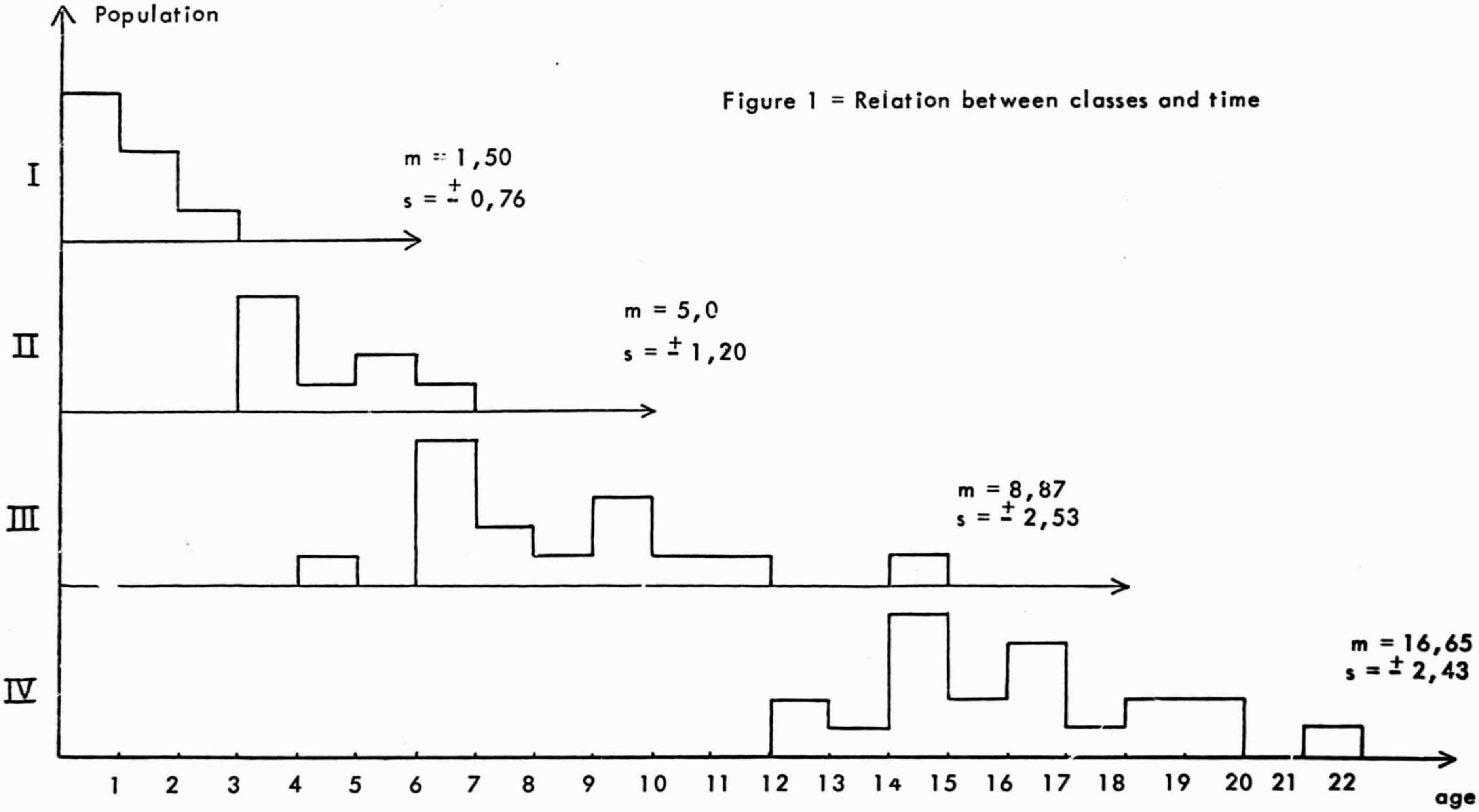

Figure 1 = Relation between classes and time

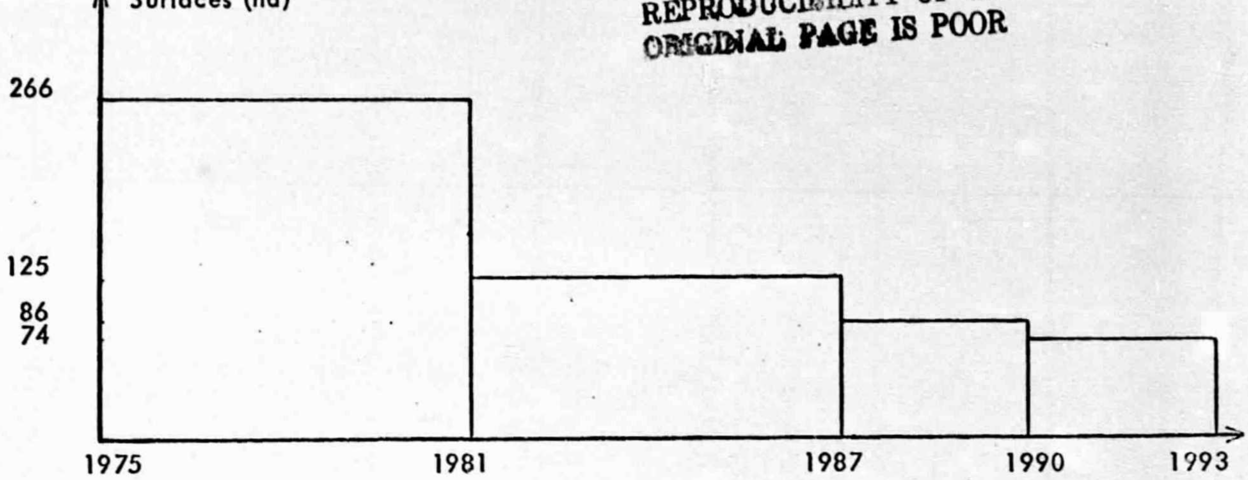

Class	IV	III	II	I
Age	more than 13 years	12 - 11 - 10 - 9 - 8 - 7 -	6 - 5 - 4 -	3 - 2 - 1
Density	312	276	282	267
Trees	82 900	34 500	24 200	20 000

Figure 2 : Global forecast of available timber

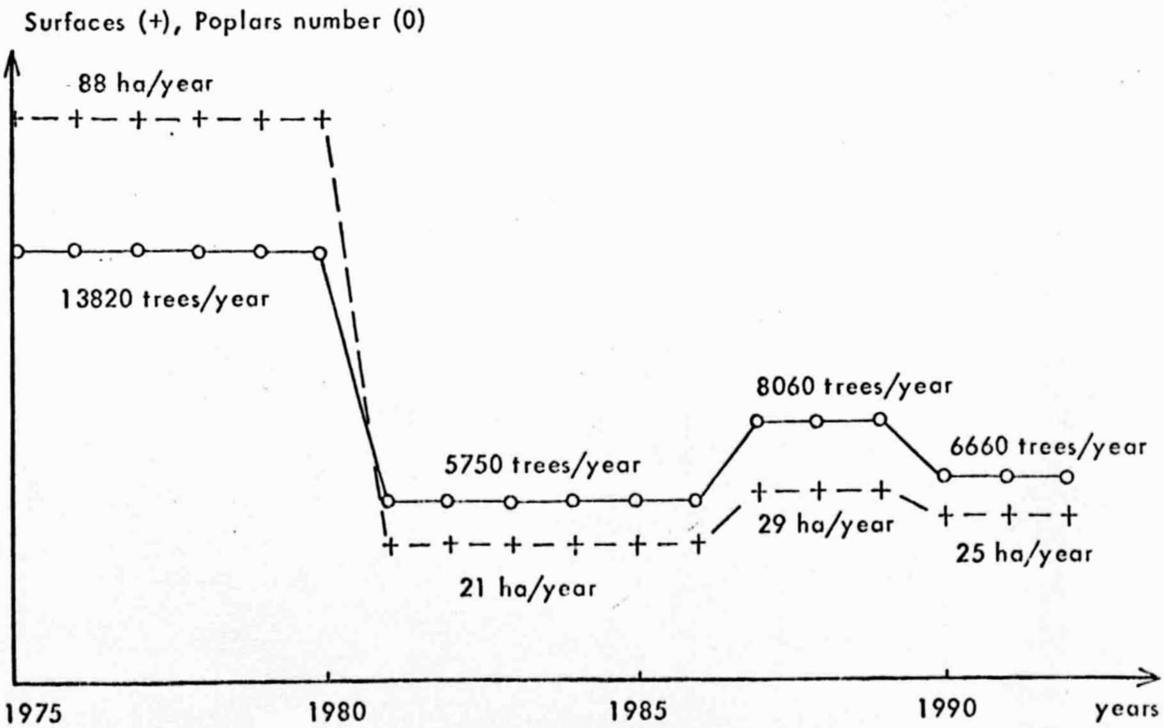

Figure 3 : Global forecast of available timber/year

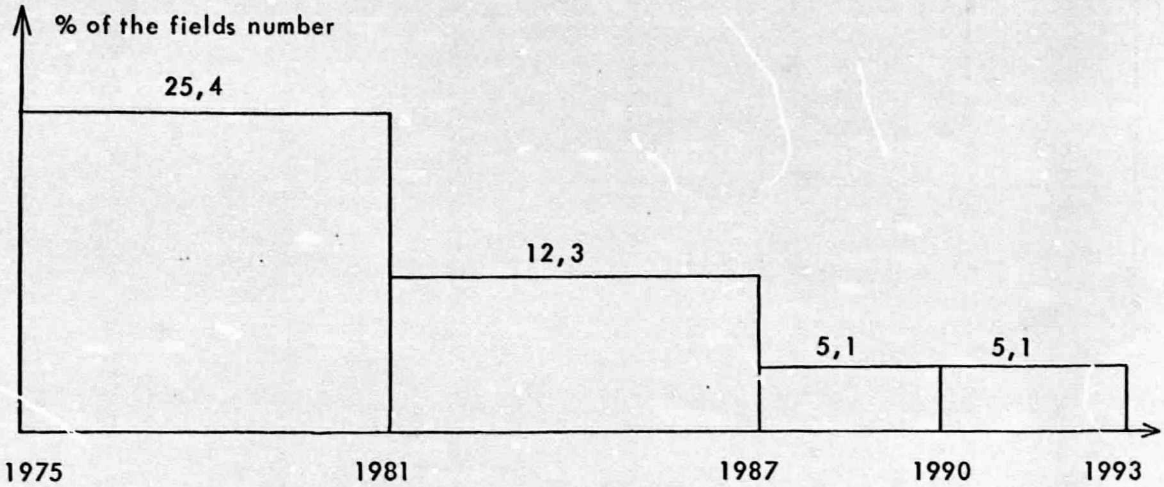

Figure 4 : Forecast of I 214 available timber

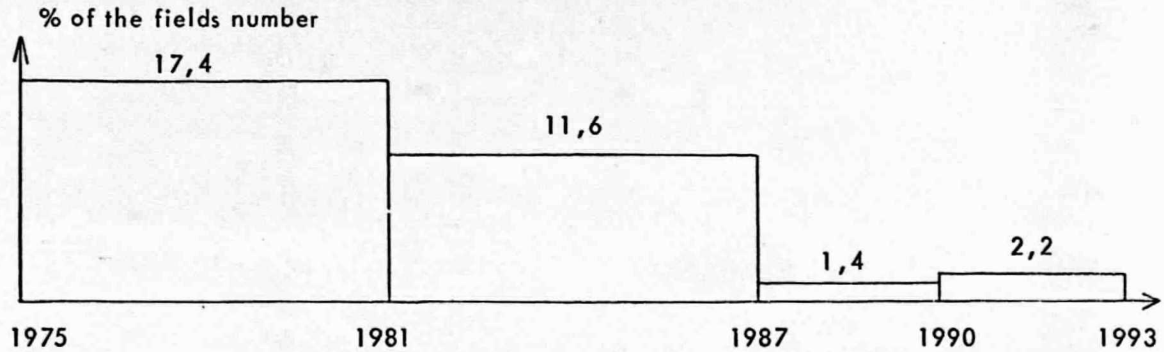

Figure 5 : Forecast of Robusta available timber

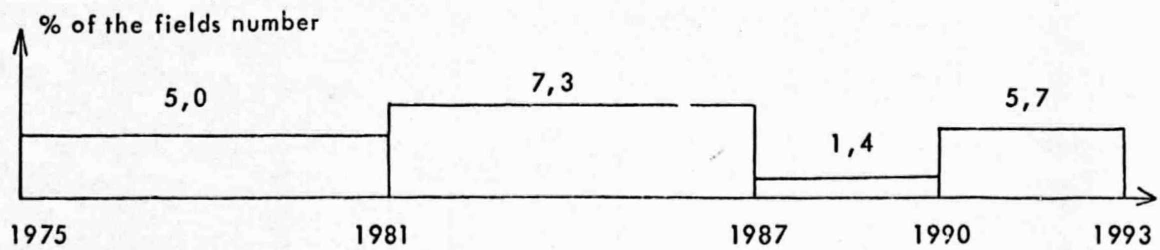

Figure 6 : Forecast of the others cultivars available timber

CHAPTER 2

ESTIMATION OF TIMBER VOLUME
IN A POPLAR PLANTATION BY REMOTE SENSING

by G. FLOUZAT *

Abstract :

The evaluations of timber volume are given by definition of biometrical connections between the mean surface of poplars crowns in a plantation and the mean circumference of the same trees take at 1,30 m.

PRINCIPLE

The estimation of a standing timber volume is done by elaboration of relationships between a biometrical characteristic of the studied trees and a remotely measurable parameter. That enables to know a characteristic of the trees by remote sensing.

In the case of poplar plantations, the remotely measurable parameter is the cover percent of vegetation to the ground. The geometrical position of trees makes the mean surface of crown computable.

Three methods can give this measurement :

- microdensitometry
- photogrammetry
- model comparison

* Centre d'Etude Spatiale des Rayonnements
9, avenue du Colonel Roche
31029 TOULOUSE CEDEX

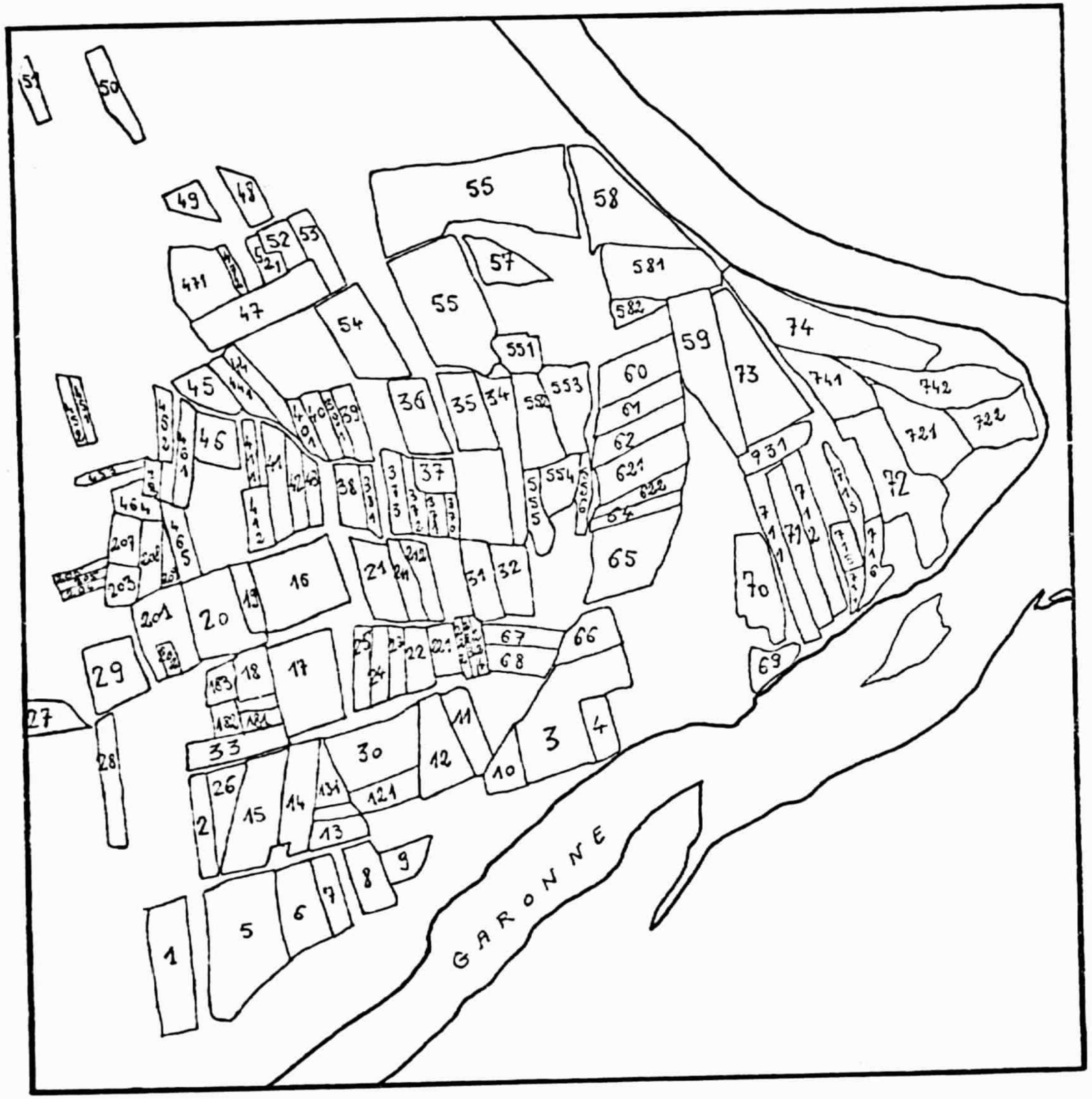

SAMPLING AREA n° 1

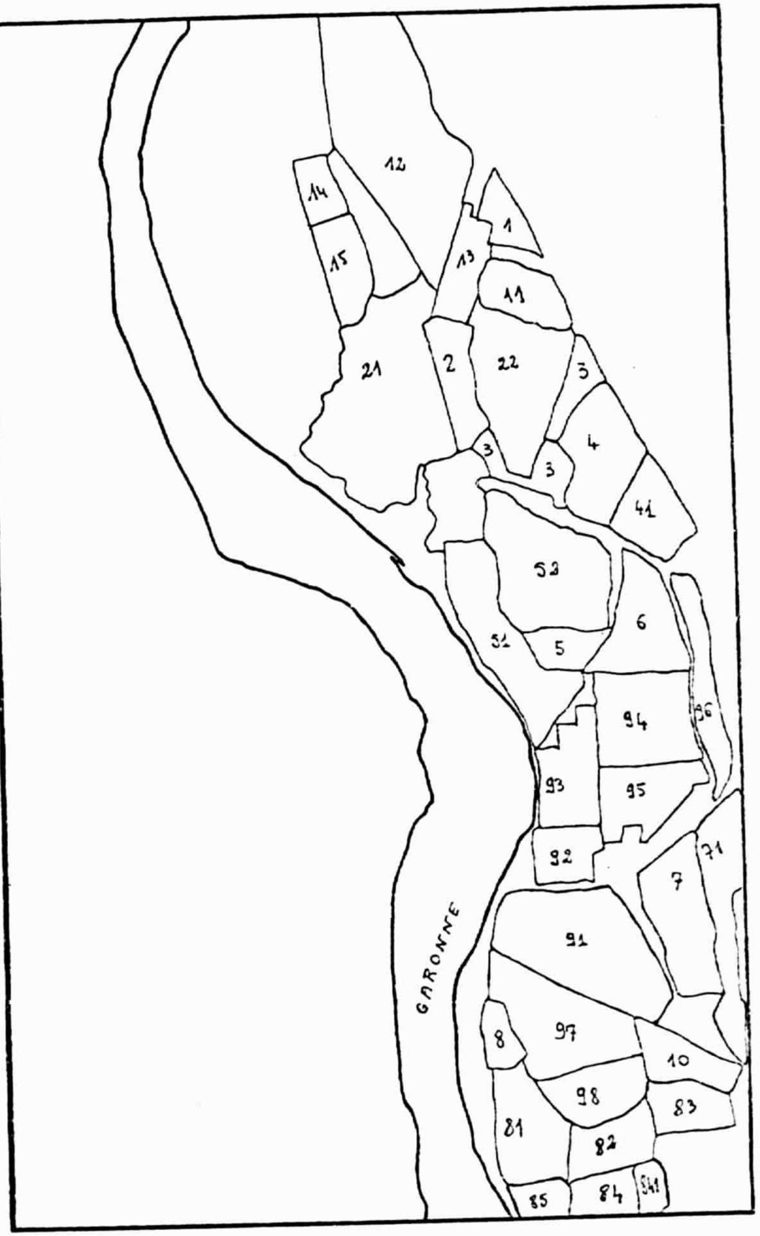

SAMPLING AREA n° 2

When the cover percent is obtained, the figure 1 shows corresponding surface of the mean surface (C.S.) It is this data which is used to be connected with a tree character.

SAMPLING AREAS

The retained biometrical parameter is the circumference at 1,30 m level (c) . Therefore, it is necessary to know the C - variation when C.S. in varying.

For this objective, C-measurements are made on the ground at the same fields that C.S. measurements are made with IRC photographs.

Figures "Sampling area n° 1" and "Sampling area n° 2" (scale : 1/10 000) localize the ground works.

In these plantations, the following data are collected :

- cultivated variety
- circumference (1,30 m)
- cover percent estimation

These informations are completed with plantation density, plantation mode, plantation age and, if possible, the mean height of trees.

RELATIONS BETWEEN CROWN SURFACE AND CIRCUMFERENCE

Data are classed to group the measures coming from a same plantation type for a same cultivated variety.

Then, the relationships between crown surface and circumference at 1,30 m are established. The figure 2 gives an example for I 214 cultivated variety with a 204 p/ha density.

The remote sensing measure, therefore, can give a characteristic of the tree which is directly connected with the stem volume.

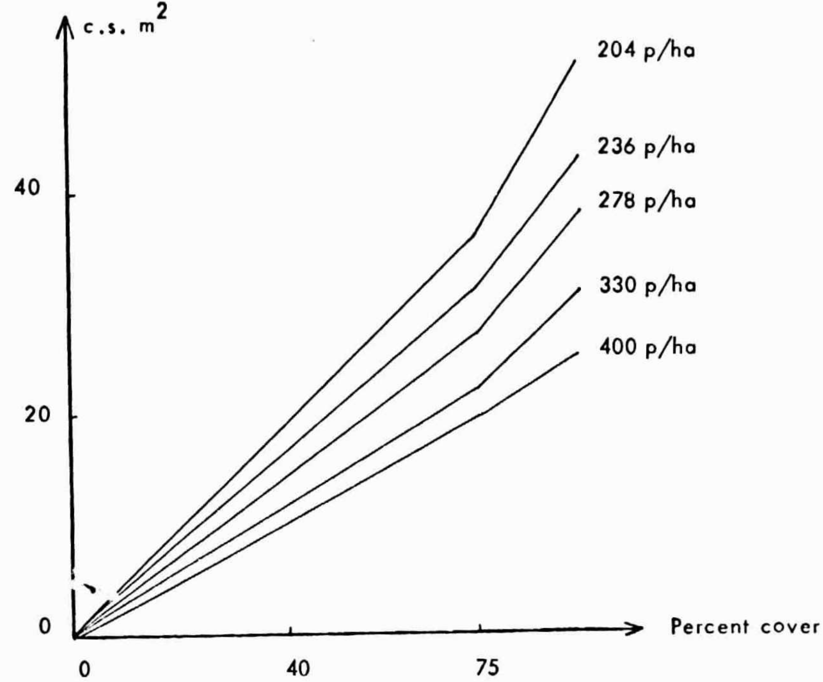

Figure 1

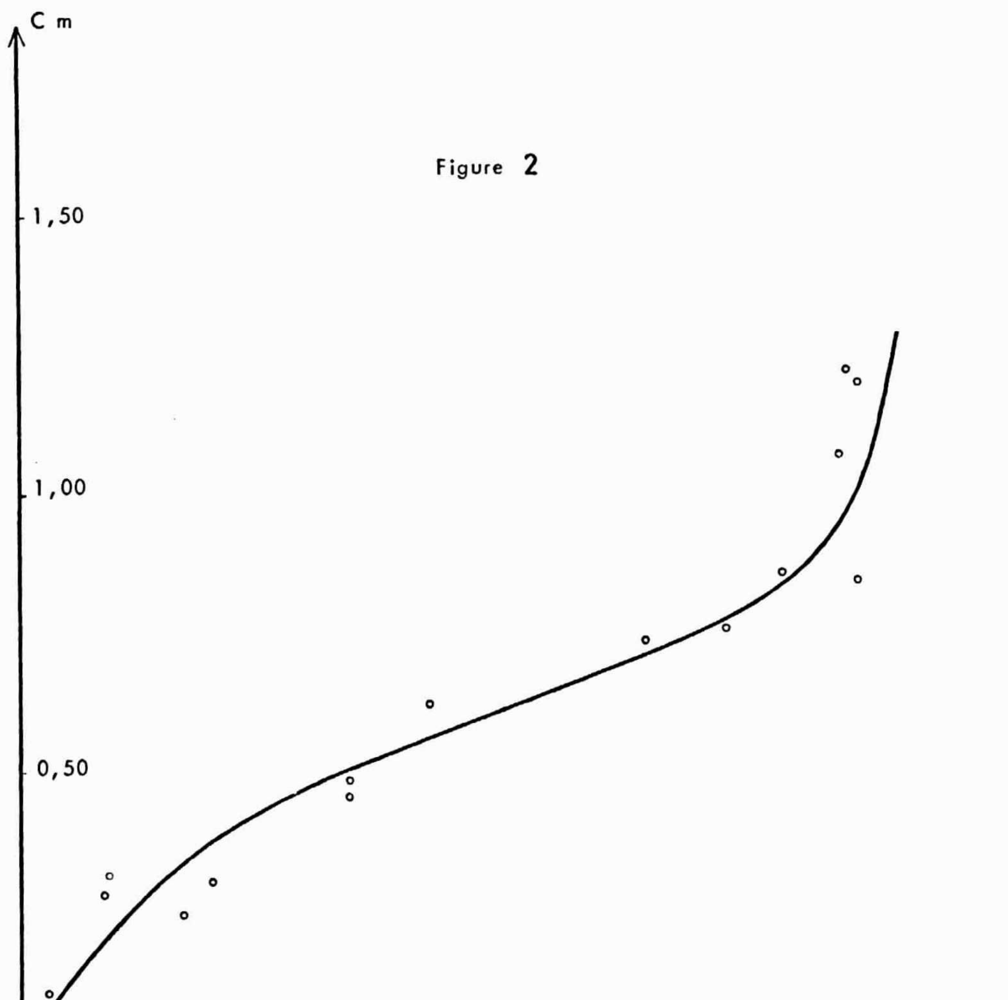

Figure 2

Relation between crown surface (c.s.) and circumference (C)
for 1 214 plantations at 204 p/ha density.

CHAPTER 3

DIFFERENT CLASSIFICATION METHODS APPLIED TO LANDSAT IMAGERY

(AGRESTE test-site n° 4)

by P. CASSIRAME*

Abstract :

Several classification methods are applied to Landsat-2 imagery on Agreste test-site n° 4. Supervised and unsupervised methods are used. The comparison of results are shown and also the computing time consomed by these methods.

The Landsat-2 Imagery is used to compare the efficiency of different classification methods evolued at the C.E.S.R. Two are supervised : Sebestien classifier and Fix-Hodges classifier. The thirdth is unsupervised : the mobile centre clustering technique using the following distances : Euclidean, chi square and Mahalanobis. Finally a regularisation is carried out to smooth the results.

* Centre d'Etude Spatiale des Rayonnements
9, avenue du Colonel Roche
31029 TOULOUSE CEDEX

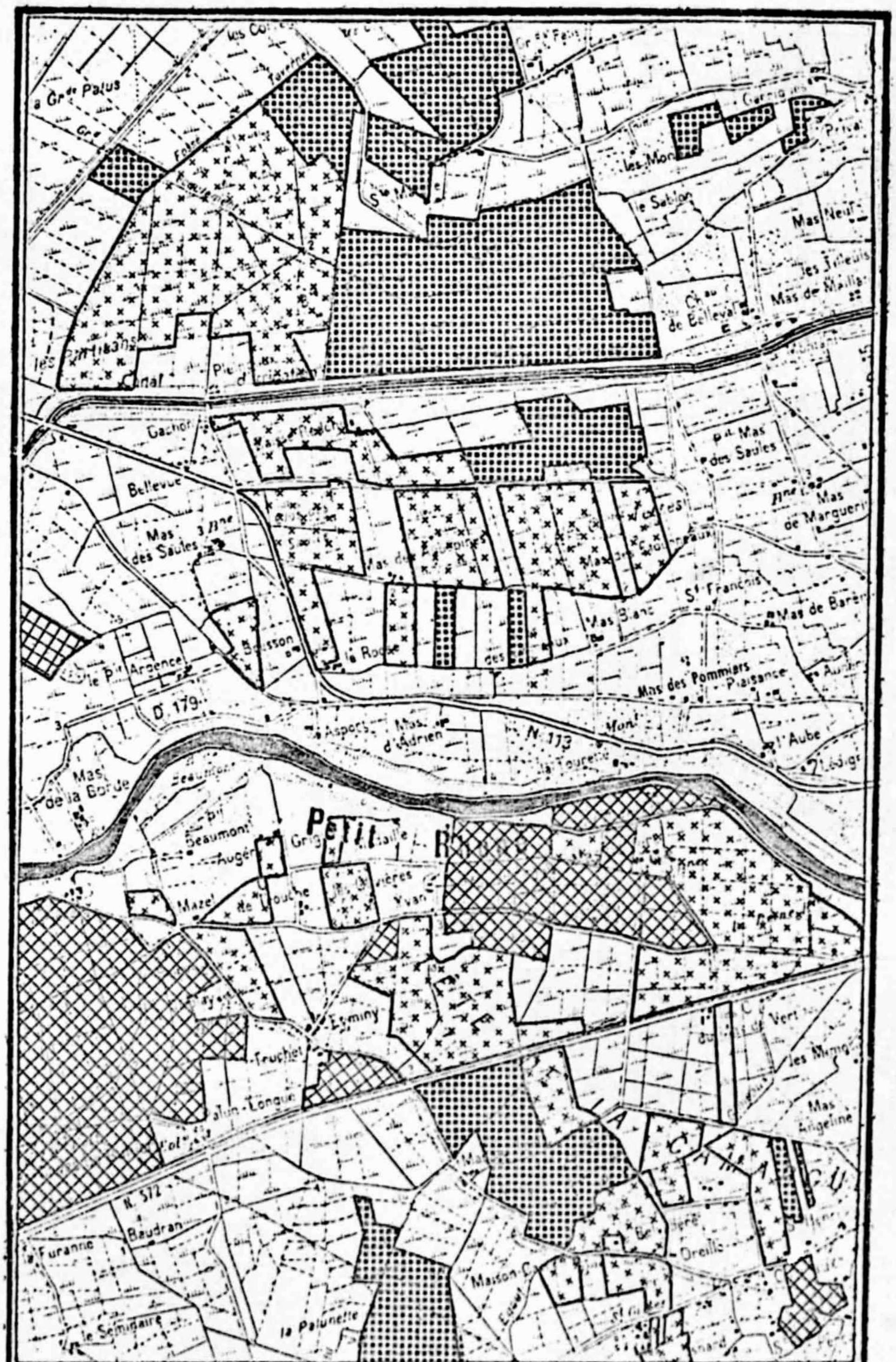
le Sablon
Bellevue
Mas des Saules
pt Mas des Saules
Mas de Marguerit
St Francis
Mas Blanc
Mas de Barên
Mas des Pommiers
Plaisance
l'Aube
le Pt Argence
D. 179
N. 113
Mas de la Borde
Beaumont
Petit
Mazel
Yvan
Eyminy
Truchet
Mas Angeline
N. 572
Baudran
Furanne
le Séminaire
la Palunette
Maison

Figure 1

The studied scene is a part of the Agreste test-site n° 4. It is an area of 120 x 120 pixels (corresponding to 6,7 km x 9,5 km) near Arles City and crossed by the river "Petit Rhône". Main field categories in this region are ricefields, Vineyards and Wheatfields. We only use images recorded on the 11th of August 1975.

Figure 1 shows the location of some field categories in this region : ricefields in dark grey, vineyards in medium grey and wheatfields in light grey.

SUPERVISED METHODS

These methods are based on a priori knowledge of prototype classification. Sebestien classifier uses the discriminant function d :

$$d^2 (x, y_k) = |S_k|^{1/n} \left((x - E(y_k))^t \; S_k^{-1} \; (x - E(y_k)) + n \right)$$

with Y_k = set of k^{th} prototype pixels

S_k = covariance matrix of y_k

n = number of bands

E = expectation function.

Fix-Hodges classifier generalizes the K - Nearest - Neighbour rule.
Euclidean weighted distance is used : $d^2 (x_1, x_2) = \sum_{i=1}^{n} \lambda_i (x_{1i} - x_{2i})^2$
The principle consists to choose λ_i to get maximum of well classified prototypes.
The process starts with $\lambda_i = 1/\sigma_{ii}2$, $\sigma_{ii}2$: total variance of prototypes in band i.
Then λ_i varies in $(1/\sigma_{ii}2 - \Delta\lambda , 1/\sigma_{ii}2 + \Delta\lambda)$ where $\Delta\lambda$ is prespecified.

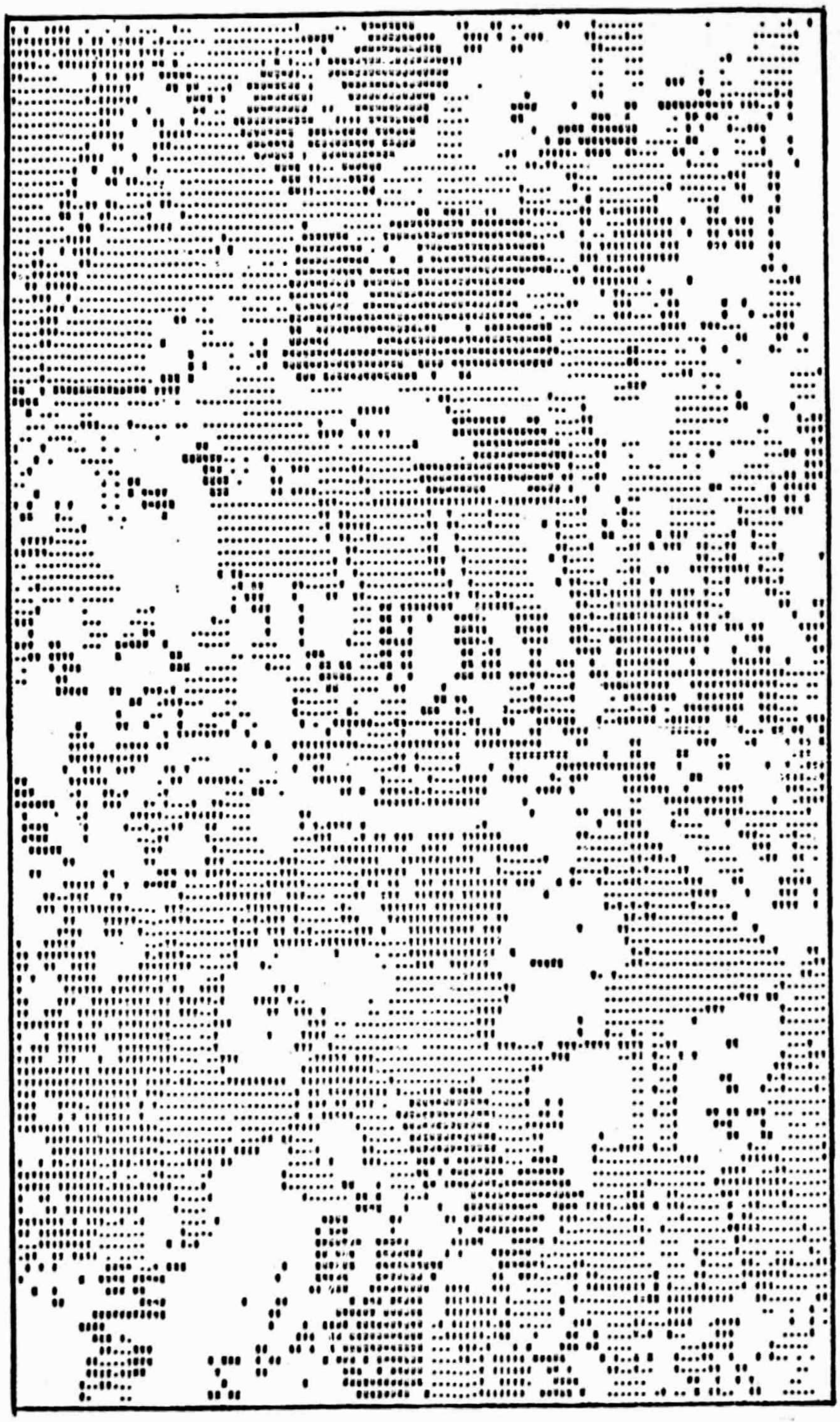

SEBESTIEN CLASSIFIER

Fig. 2

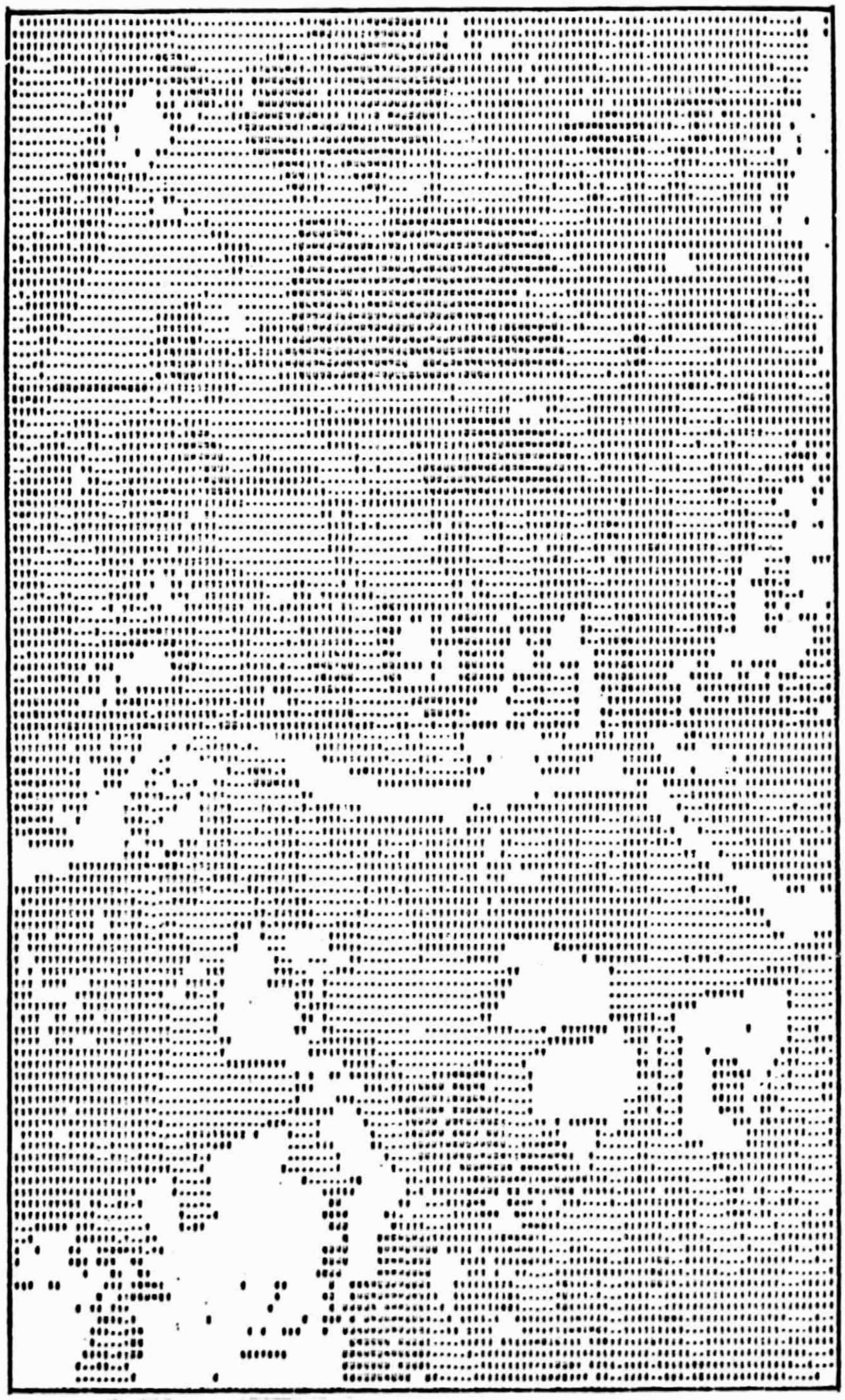

FIX-HODGES CLASSIFIER

Fig. 3

Method \ Location	"Les Pebrières" ricefield	"Huit - clos" ricefield	"Mas du Tort" ricefield	"Mas de Vert" Vineyard	"D^{ne} de la Reine" Wheatfield
Owner estimation	43	189	95	84	111
Sebestien classifier	47	195	86	82	113
Fix-Hodges classifier	48	198	71	73	117

Table I

Table I shows areas (ha) of some fields calculated by the two methods. Sebestien classifier is better than Fix-Hodges method with regard to owner estimation.

Processing time is 2s (CP time CDC 7600) for both methods.

UNSUPERVISED METHOD

The principle of mobile centre clustering technique was described in a previous quaterly report (March-June 1975), the distances used are the following :

euclidean : $d^2(x_1, x_2) = \sum_{i=1}^{n} (x_{1i} - x_{2i})^2$

chi square : $d^2(x_1, x_2) = \sum_{i=1}^{n} k \left[\frac{x_{1i}}{\sum^{n} x_{1i}} - \frac{x_{2i}}{\sum^{n} x_{2i}} \right]^2$

Mahalanobis : $d^2(x,y) = ((x-E(y))^t \, S_i^{-1} \, (x-E(y))$

SMOOTHING

The principle of regularisation consists to affect to a pixel, after classification ; the majority class of pixels in his neighbourhood (fig. 7)

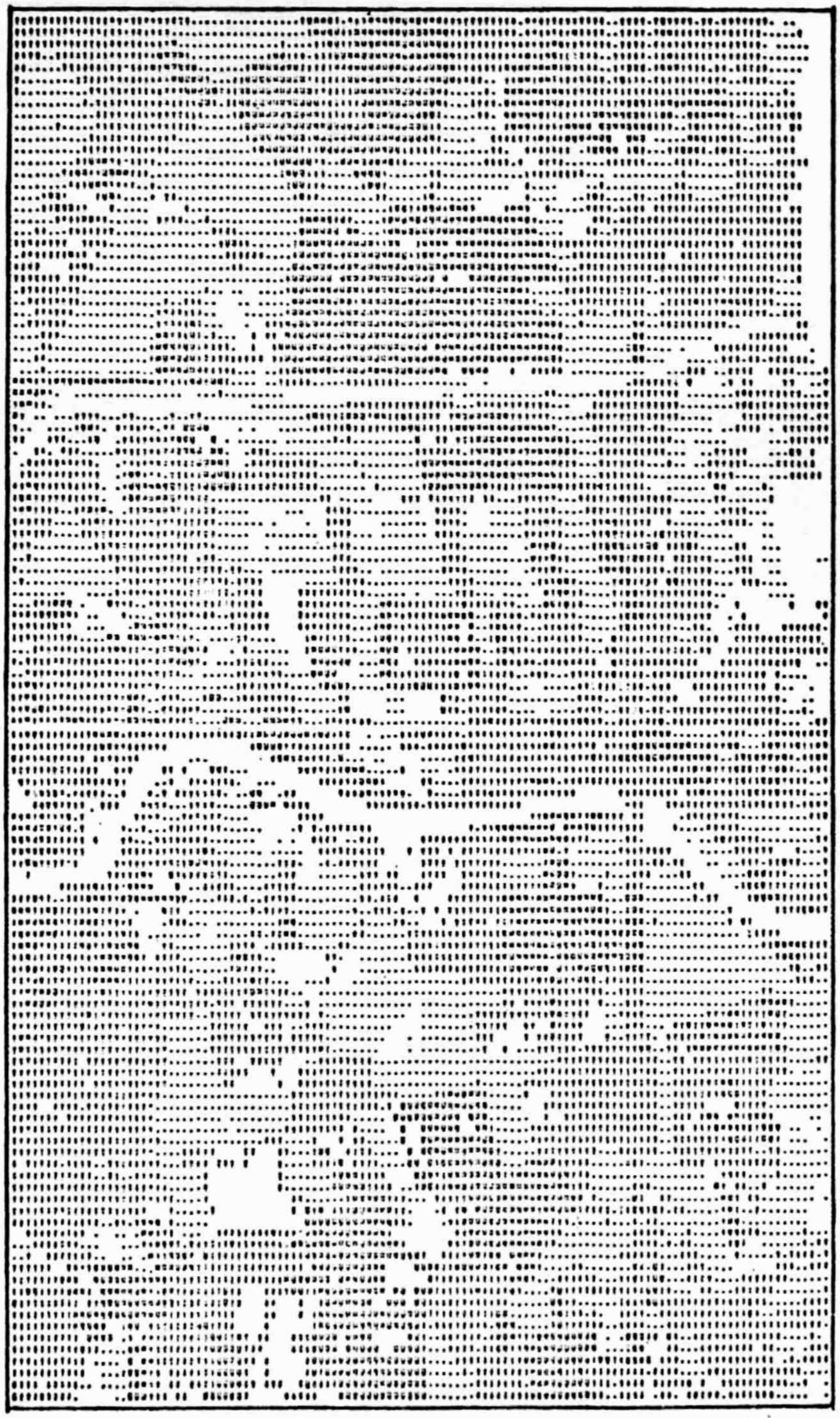

MOBILE CENTRE TECHNIC

EUCLIDEAN DISTANCE

Fig. 4

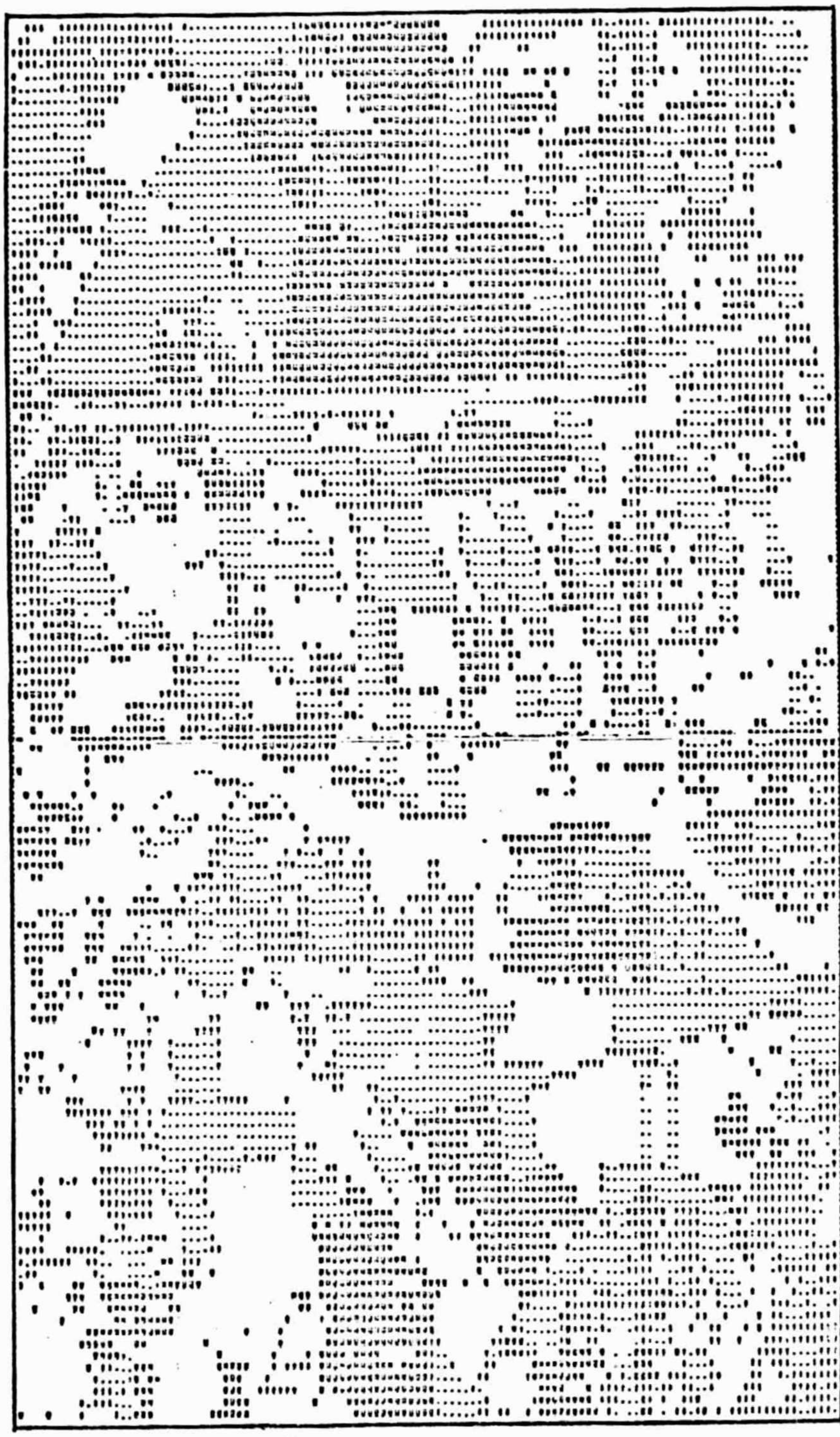

MOBILE CENTRE TECHNIC
CHI SQUARE DISTANCE

Fig. 5

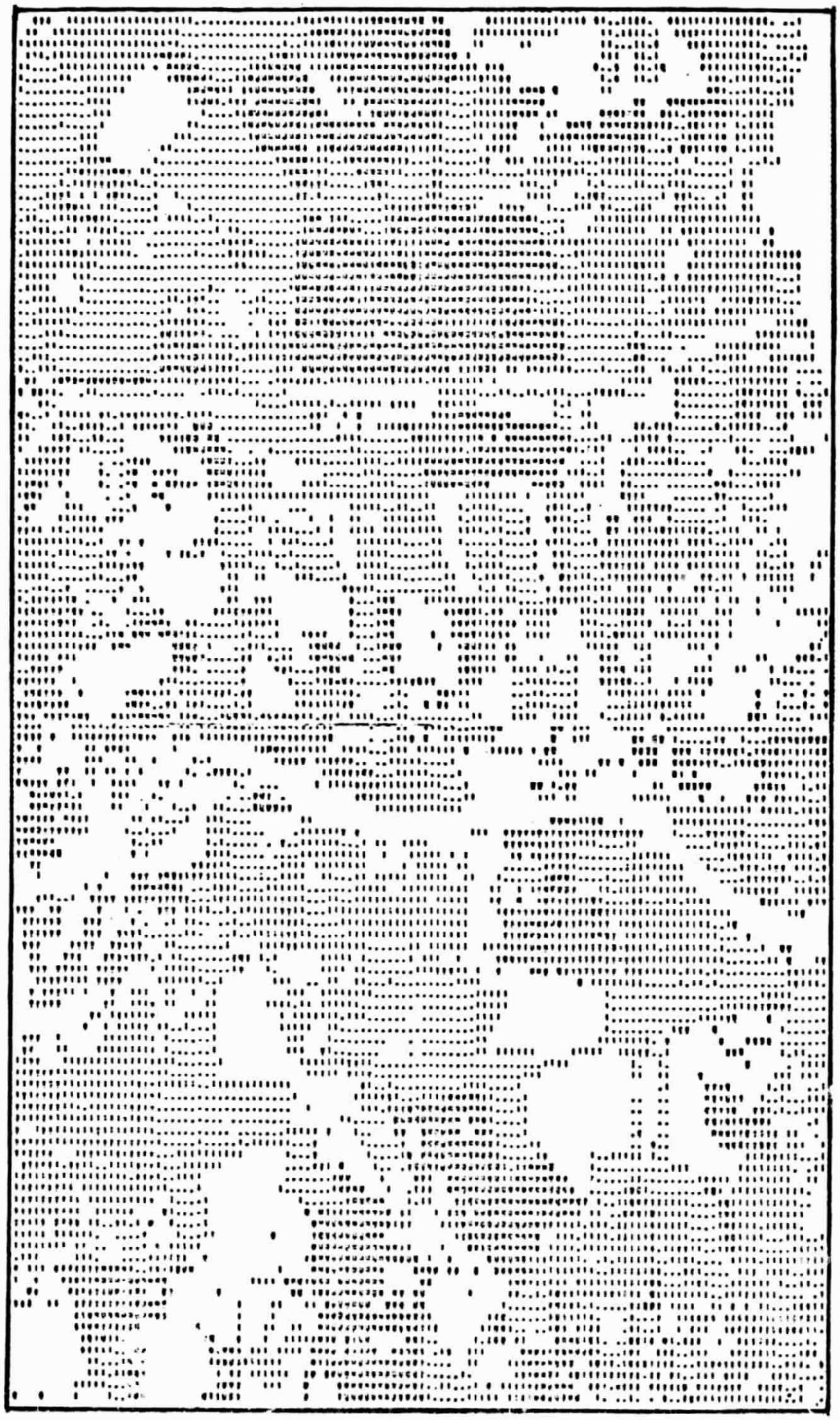

MOBILE CENTRE TECHNIC

MAHALANOBIS DISTANCE

Fig. 6

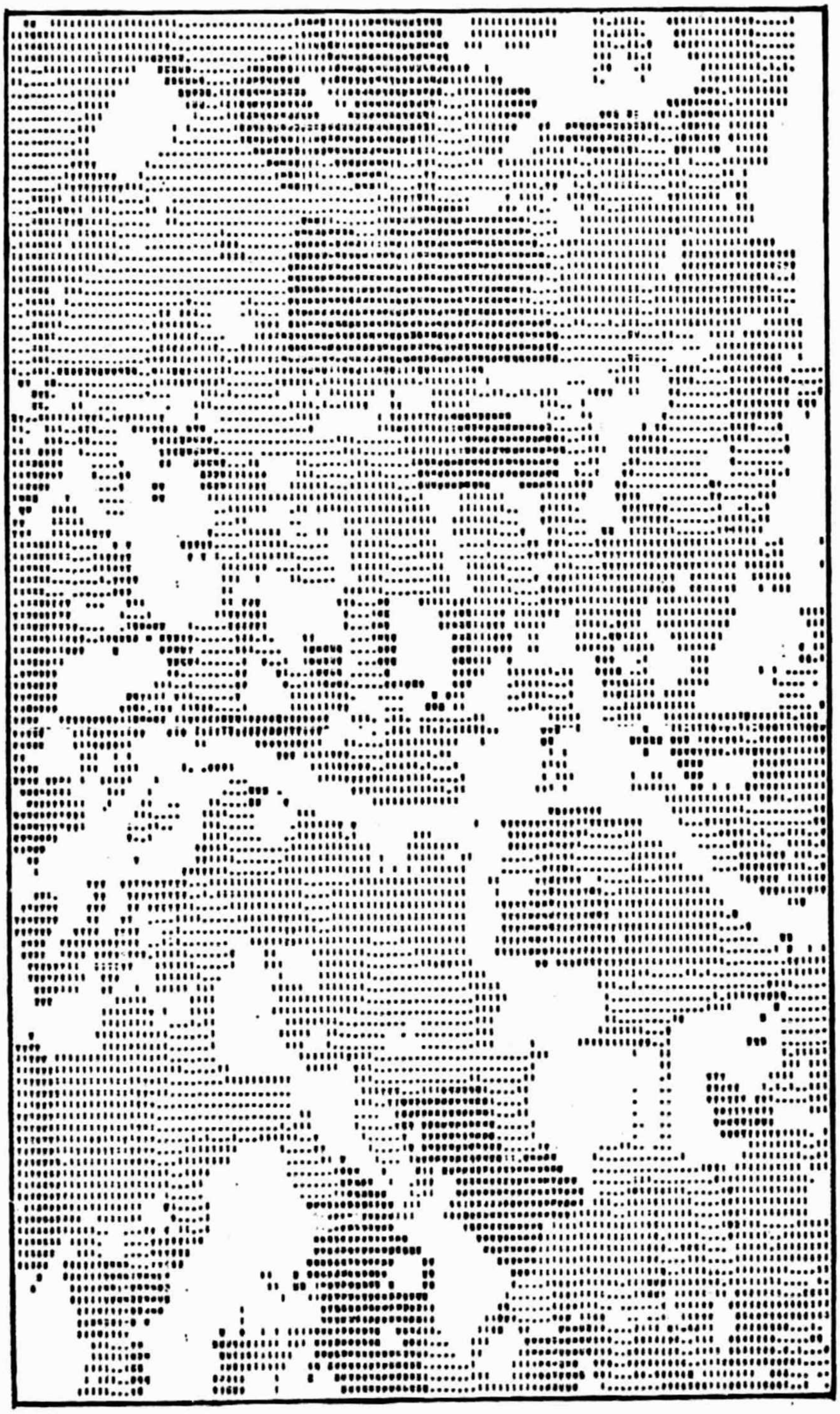

SMOOTHING of Figure 6

Fig. 7

Method \ Location	"Les Pébrières" ricefield	"Huit-Clos" ricefield	"Mas du Tort" ricefield	"Mas de Vert" vineyard	"D^{ne} de la Reine" Wheatfield
Owner estimation	43	189	95	84	111
Clustering method euclidean distance	46	190	94	72	119
id. χ^2 distance	45	157	66	77	120
id. Mahalanobis distance	42	157	87	73	88

Table II

The comparison of table I and table II indicates that supervised methods are better than clustering technique. Meanwhile some details are pointed out by the mobile centre technique such the partition of wheatfields into two subclasses corresponding to different parcels (fig. 6) processing time is about 10 s.

CONCLUSION :

Landsat imagery is sufficient for large fields discrimination but small parcels such market-gardens are not discernible, given the importance cost of mobile centre technique it is better to use supervised methods.

CHAPTER 4

SEVERAL GREY-LEVEL MANIPULATIONS
LEADING TO AN ALGORITHM OF EDGE DETECTION

by J. QUACH (CESR)

Abstract

We present several image processings using discrete operators to smooth, sharp or detect edges of digital pictures.

We improve these operators used for many years by combining the gradient, the mean of grey-levels on well defined neighbourhood, the distance to the mean ...

We use then one of those combinations to extract edges of an image.

I - INTRODUCTION

We process an IRBW image of ricefields in Camargue (Agreste test site n° 4).

II - DEFINITION OF SOME BASIC TERMS

. A point of a digital picture is defined by his coordinates (i,j) and his grey-level x.

. We shall use two kinds of neighbourhood for the point (i,j)

$V_1(i,j) = (i,j)\ ;\ (i+1,\ j)\ ;\ (i,j+1)\ ;\ (i-1,\ j)\ ;\ (i,j-1)$

$$\begin{array}{ccc} & x & \\ x & . & x \\ & x & \end{array} \qquad \begin{array}{ccc} & b & \\ c & x & a \\ & d & \end{array}$$

and

$V_2(i,j) = (i,j)\ ;\ (i+1,\ j)\ ;\ (i,\ j+1)\ ;\ (i-1,\ j)\ ;\ (i,j-1)\ ;\ (i+1,\ j+1)\ ;\ (i-1,\ j+1)\ ;$
$(i-1,\ j-1)\ ;\ (i+1,\ j-1)$

$$V_2(i,j) \qquad \begin{array}{ccc} x & x & x \\ x & . & x \\ x & x & x \end{array} \qquad \begin{array}{ccc} f & b & e \\ c & x & a \\ g & d & h \end{array}$$

. In this paper, an image processing consists to replace the grey level of (i,j) : x by a new grey level dependent of the grey levels on V_1 (i,j) or $V_2(i,j)$ i.e. $_{V1}(x)$ or $_{V2}(x)$.

III - THE BASIC OPERATORS

They are generally operators of the differential geometry that we have discretized to process digital pictures.

We'll then distinguish derivative operators (first and second order) showing contrasts, intensity variations and integrate operators leading to a smoothing.

We may apply these operators to the neighbourhoods V_1 or V_2

MOYENNE : (see Fig. 1) Integrate operator computing the arithmetic mean of the grey levels of (i,j) and his neighbours

on V_1 : $RMOY(i,j) = (a+b+c+d+x)/5$

on V_2 : $RMOY(i,j) = (a+b+c+e+f+g+h+x)/9$

ECART : Derivative operator (second order) computing the difference between the grey level x of (i,j) and the mean of the neighbours

$DIF(i,j) = x - RMOY(i,j)$

DIF (i,j) may be negative.

CONTRASTE : We increase the initial grey level by the value of ECART at this point

$$AC(i,j) = A(i,j) + DIF(i,j) = x + DIF(i,j)$$
$$= 2x - RMOY(i,j)$$

A point clearer than his neighbours is becoming more clear.

GRADIENT : Derivative operator (first order). We discretize the usual gradient grad f = $(\frac{\partial f}{x}, \frac{\partial f}{y})$; here therefore we take grad A = (U,V) with, on V_1 only

$U = a - x$

$V = b - x$

We calculate :

. Euclidean norm of grad A (see fig. 2)

$Gx(i,j) = (U^2 + V^2)^{1/2}$

. Argument of grad A

$$THETA(i,j) = \frac{180}{\pi} \text{Arctan}(U/V) \quad \text{if } V \neq 0$$
$$= 0 \quad \text{if } V = 0$$

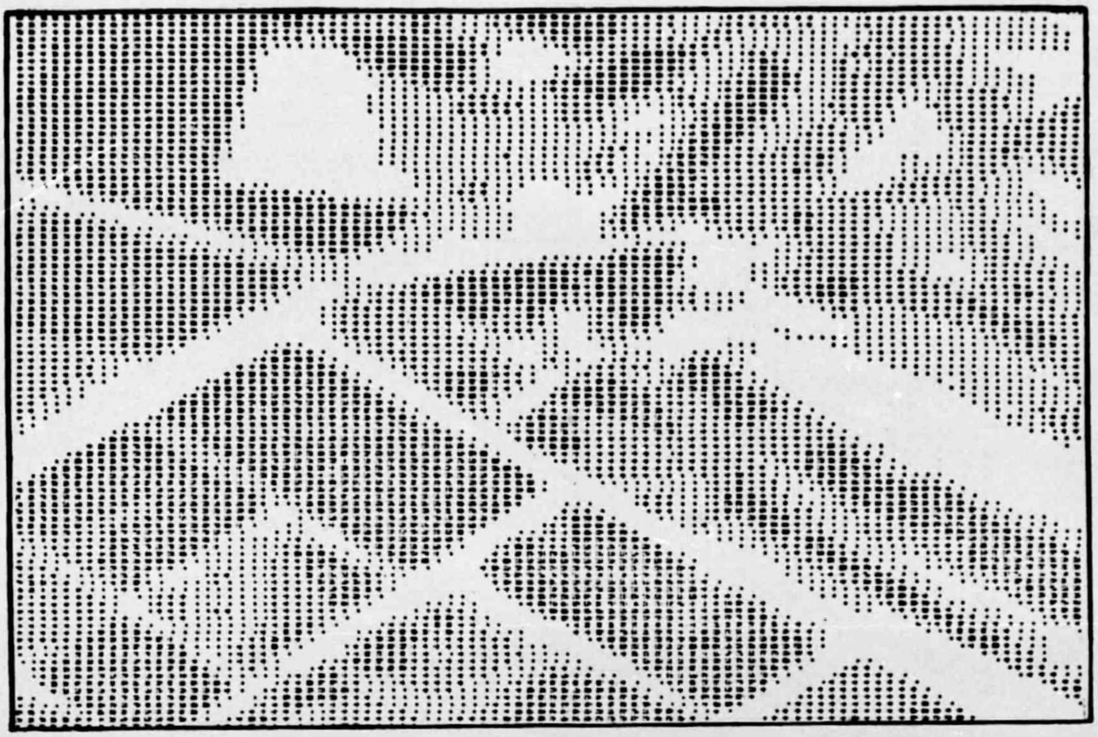

Fig. 1 - Smoothing by "MOYENNE"

Fig. 2 - Euclidean norm of the Gradient

IV - MIXING OPERATORS AND EDGE DETECTION

We use the difference of behaviour of gradient and ECART to obtain new processing methods :

Smoothing (Fig. 3) We add the gradient to the initial image and we cut off the ECART (algebraic). This procedure applied to a cross section like Fig. 7 c will raise it in the central part of the ramps (positive radient), also at the bottom (we cut off negative ECART) and lowered at the top (positive ECART). Finally the luminous relief is globally attenuated.

Sharpening (Fig. 4) That is the inverse operation, i.e. we cut off the gradient from the initial picture and we add the algebraic ECART. Looking at the Fig. 7 c, we see that the slope will heighten while the central plateau will stay inchanged, therefore we increase the luminous relief.

Edges (Fig. 5) We follow the Eberlein-Weszka's method replacing gradient by the value :

$$\mathrm{Max}\ (0,\ Gx\ (i,j) - /DIF\ (i,j)/)$$

Therefore, we cut off the absolute value of ECART to the gradient and we reset the values to 0 if it is negative. ECART being maximum at the extremities of the slope and null in the middle, we thin the edge detection.

Edge following (Fig. 6) We intend, starting from the image obtained with the last processing (Fig. 5), to draw the edges of the initial image. Therefore, the main improvement is to make the picture function binary valued.

First the algorithm searches for the maximum of the image (i.e. the point where intensity variation is maximum), then it follows the line of minimal gradient, progressing from a point to the point of the neighbourhood V_2 which has the closest grey level ; thus we follow the crests of maximal grey levels.

One draw therefore a chain, which is stopped when a too low (with respect to the threshold) point is obtained, or too different from the last or belonging to a previous computed chain.

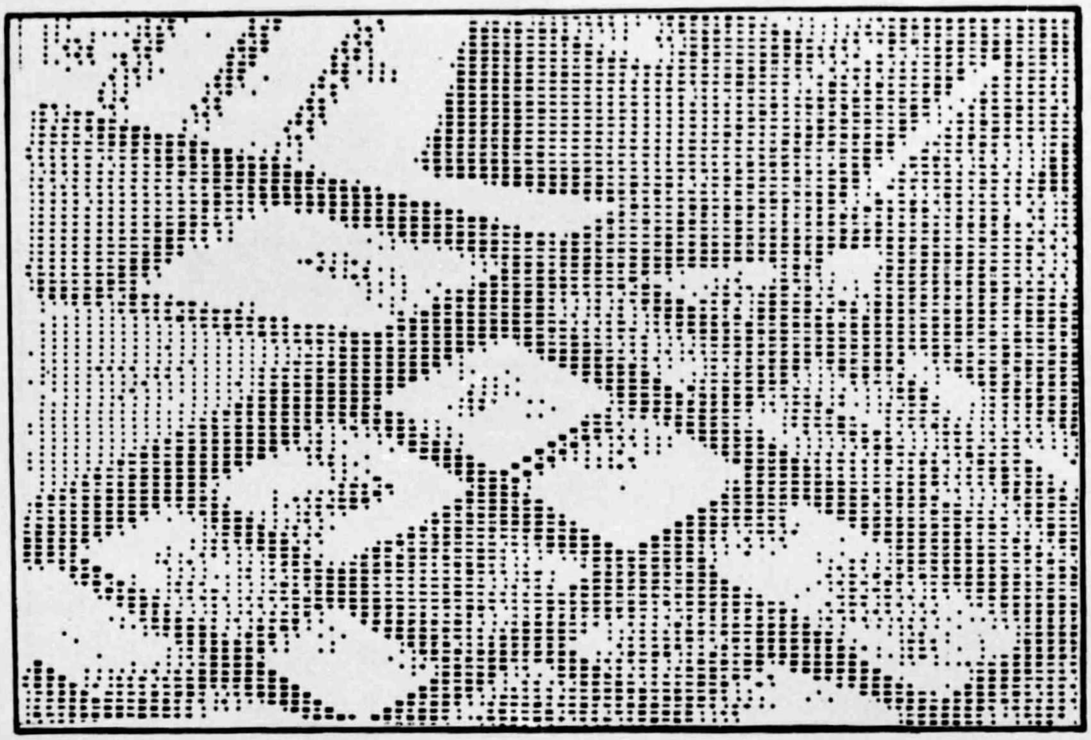

Fig. 3 - Smoothing

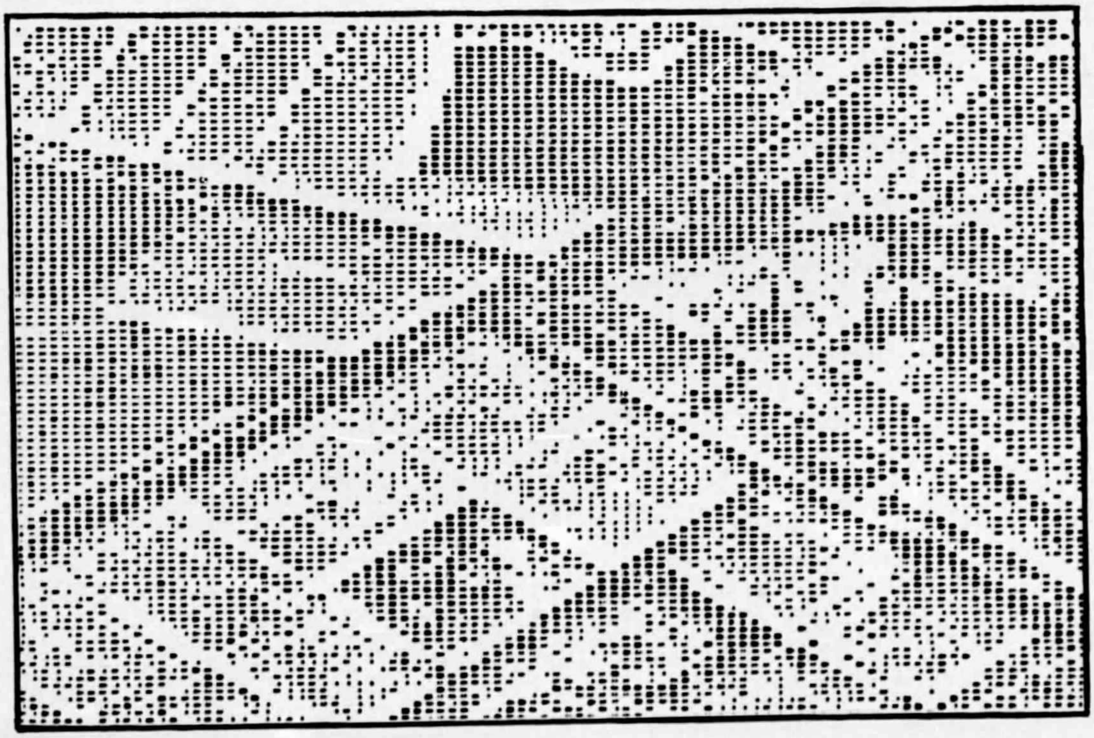

Fig. 4 - Sharpening

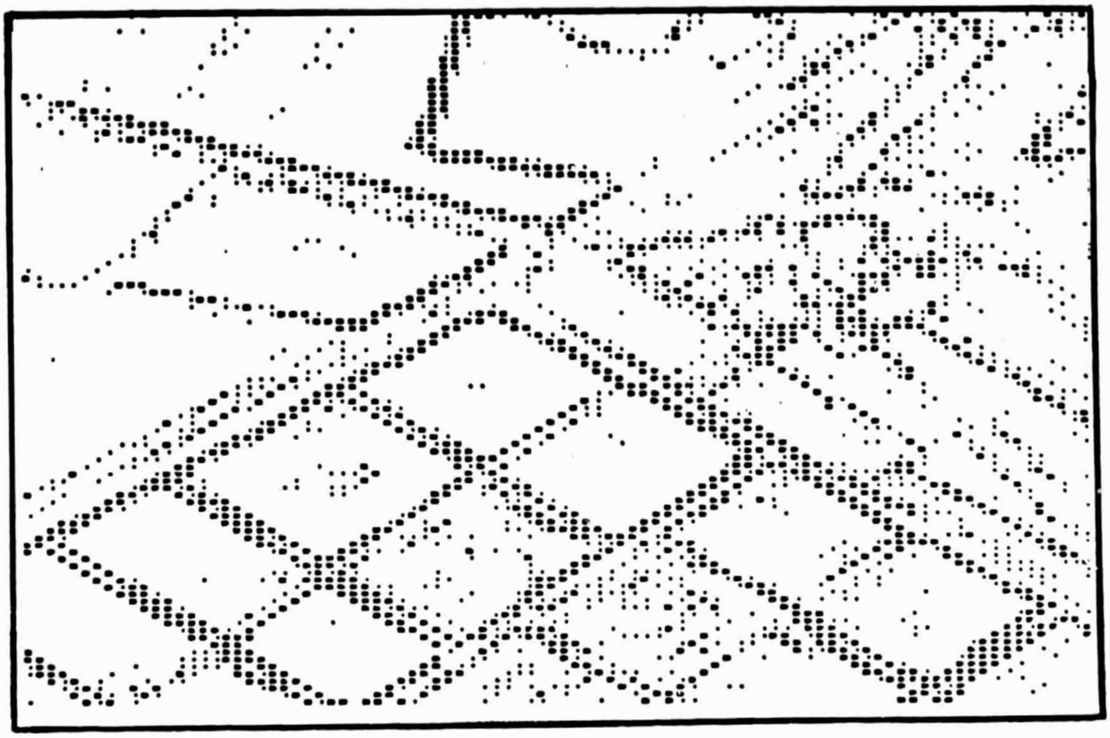

Fig. 5 - Improvement of the Gradient

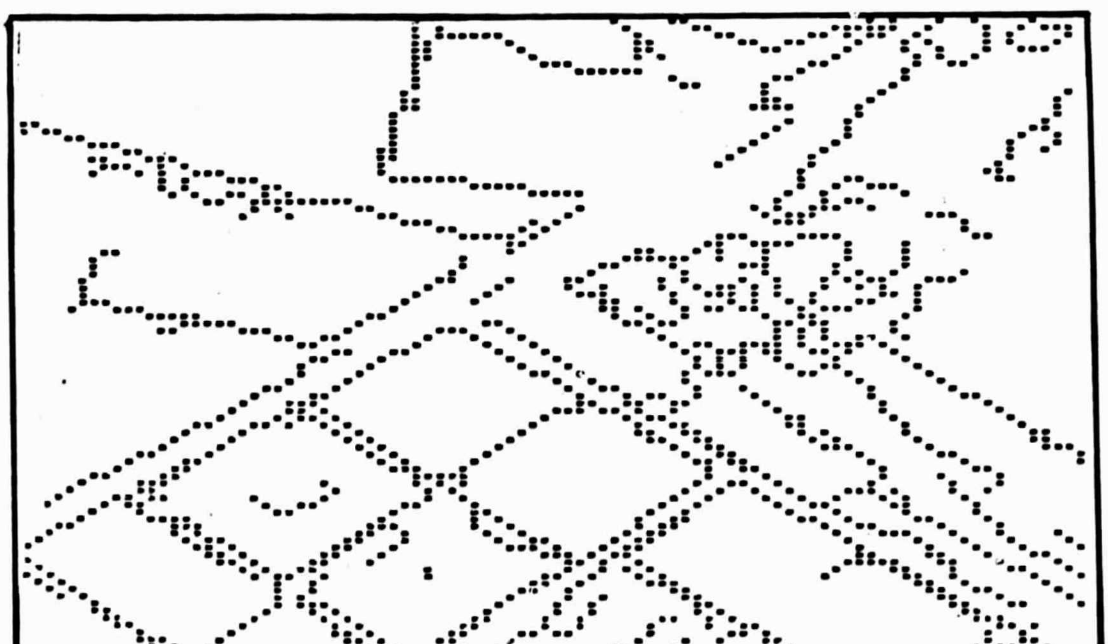

Fig. 6 - Edge detection

Note :

One must distinguish the action of GX (Norm of the gradient) and DIF (ECART or the difference between x and his neighbours).

We look at some simple examples on Fig. 7

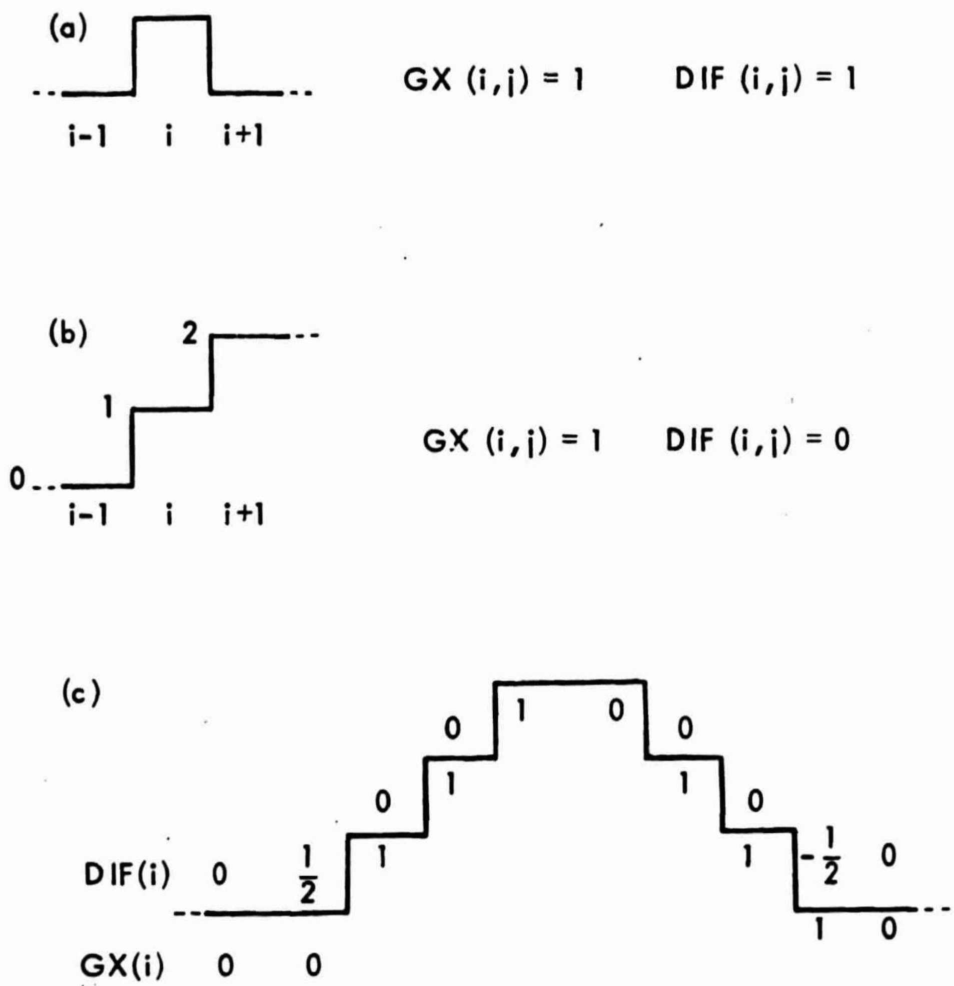

Fig. 7 Comparison between GX and DIF

The gradient behaves as a first order derivative whereas ECART looks like a second order derivative (with opposite sign).

The gradient operator reaches his maximum in the center of the ramp while ECART reaches it at the extremities, we then can use those different behaviours to find new grey levels manipulations.

We come back then to the first point of the chain and search in the opposite direction. When we attain a non suitable point, we search for a new maximum of the non processed points.

So forth untill we meet a too low maximum.

During this research, we privilege the three points of V_2 keeping the previous direction as well as possible, it is only if these points are not suitable ones that we look to the other ones of V_2.

Finally, for every point of the chain we compute the number of points of V_2 already processed, if this number exceeds the threshold we stop the chain in order to avoid the repetition of parallel edges.

Fig. 6 shows the results of this algorithm.